

Supporting Information, ESI[†]

Shape memory-assisted self-healing of dynamic thiol-acrylate networks

Walter Alabiso,^a Tiago Manuel Hron,^b David Reisinger,^a Daniel Bautista-Anguis,^a and Sandra Schlögl^{*a}

1. Supporting pictures

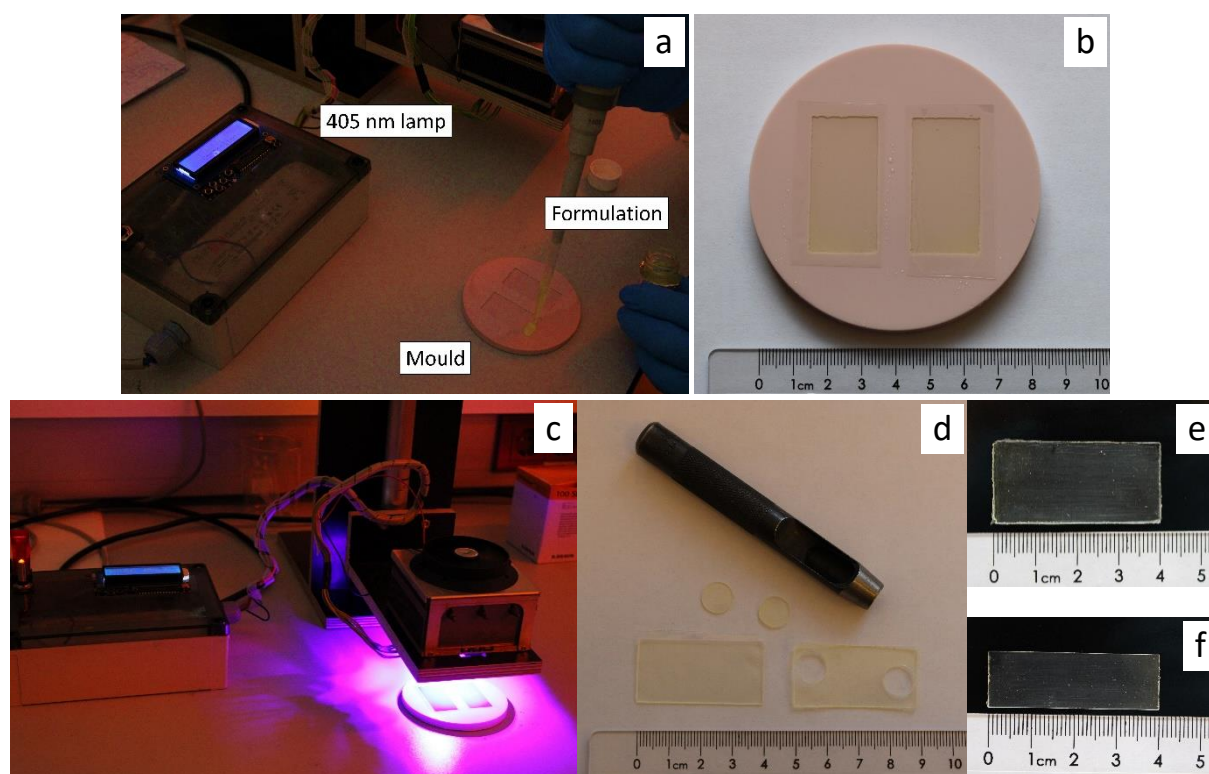


Fig. S1 – Sample preparation. **(a)** Preparation setup showing the 405 nm lamp used, the silicone mould, and the formulation being poured. **(b)** Silicone mould filled with the cured samples. **(c)** Photocuring process. **(d)** Samples for stress relaxation punched out of the original rectangle with the aid of a hole puncher. **(e)** Original sample as-removed from the mould. **(f)** Cut sample used for tensile testing.

^a Polymer Competence Center Leoben GmbH, Roseggerstrasse 12, A-8700 Leoben, Austria.

^b Montanuniversität Leoben, Otto Glöckel-Strasse 2/IV, 8700 Leoben.

* Correspondence: sandra.schloegl@pccl.at, Tel: +43 3842 402 2354

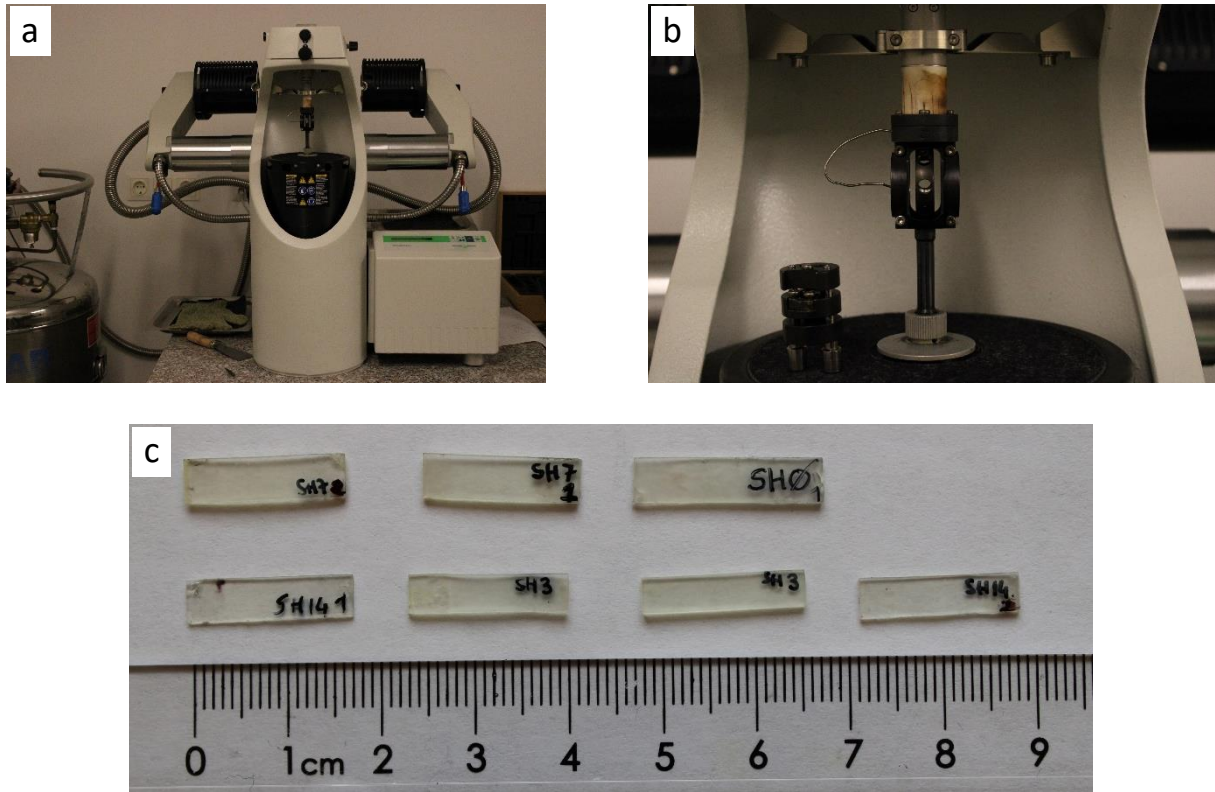


Fig. S2 – DMA experimental setup. **(a)** Picture of the device used for dynamic mechanical analysis (Mettler Toledo DMA861e analyser). **(b)** Close-up of the measuring chamber and the clamping structure used for the samples. **(c)** Examples of tested specimens for the different networks.

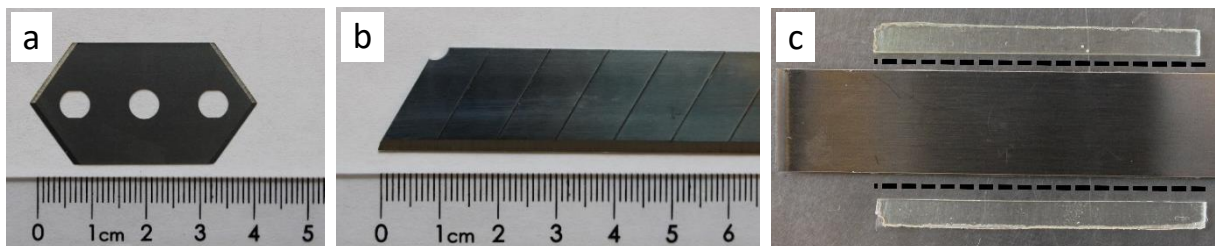


Fig. S3 – Blades used for the preparation of free-standing films by hand. **(a)** Small blade used for scratching. **(b)** Large blade from a regular office tool (reshaping of the samples and production of larger scratches). **(c)** Metal spacer used together with blade in **b** to cut out the edges of the free-standing films along the dashed black lines.

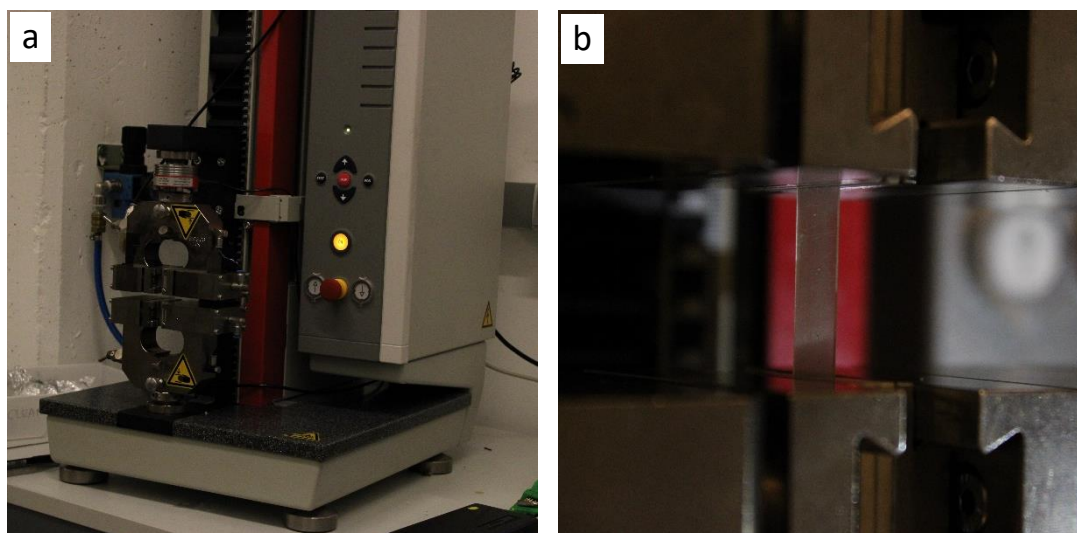


Fig. S4 – Tensile testing. **(a)** ZwickRoell (Germany) Z1.0 static materials testing machine. **(b)** Example of a specimen being tested.

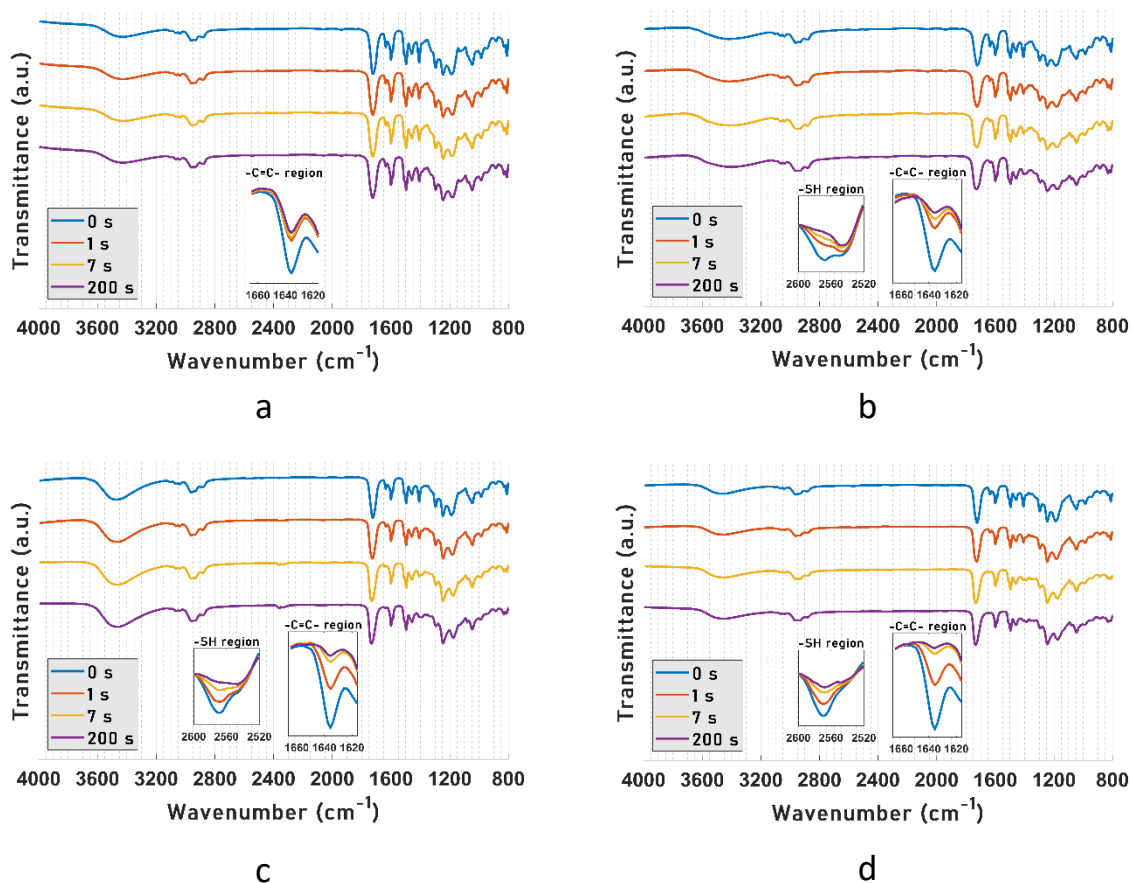


Fig. S5 – FTIR spectra and the corresponding -SH and -C=C- bands centred at 2569 cm^{-1} and 1636 cm^{-1} , respectively: **(a)** SH0; **(b)** SH3.5; **(c)** SH7; **(d)** SH14. It is evident that with a higher thiol content the conversion of acrylates reaches a higher degree more gradually. The spectra were acquired after the first 10 seconds of irradiation time and subsequently after 40, 100 and 200 seconds from the beginning of the reaction. Here, for the sake of visual clarity, only the four more representative spectra are illustrated for each network.

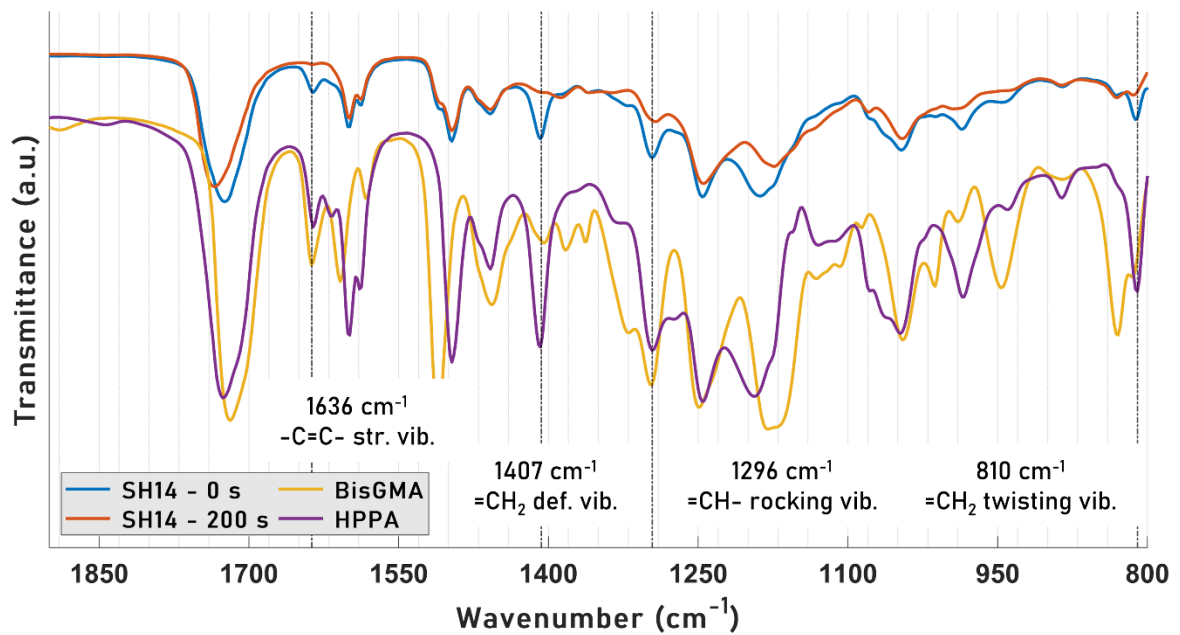


Fig. S6 – FTIR spectra for SH14 formulation (74 mol% HPPA, 12 mol% BisGMA, 14 mol% TMPMP) uncured (0 s) and after 200 s irradiation. For comparison, spectra of pure unreacted BisGMA (difunctional methacrylate) and HPPA (monofunctional acrylate) present in SH14 formulation are displayed. The characteristic IR bands¹ related to acrylate and methacrylate groups are presented in the text boxes in the figure. It is visible that the acrylate and methacrylate absorption bands are overlapping.

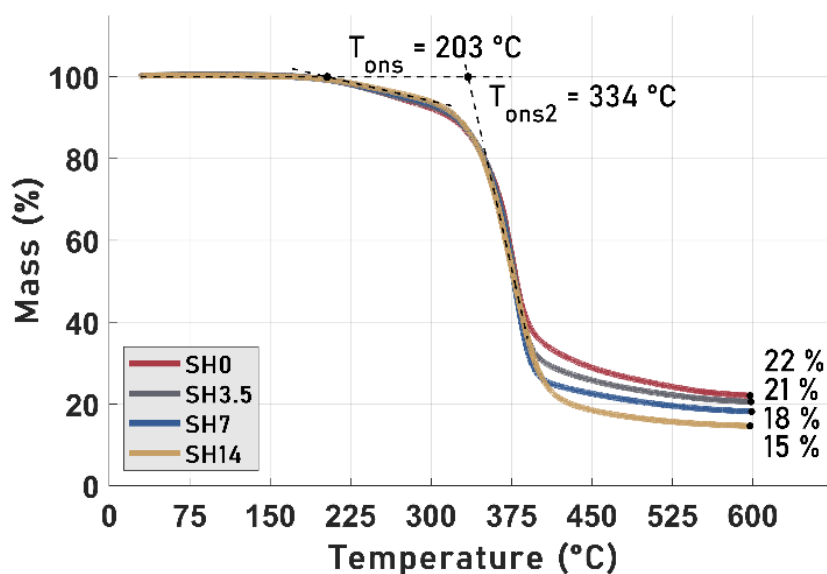


Fig. S7 – Thermogravimetical Analysis (TGA) for networks under investigation. Two onsets of mass loss can be highlighted at 203 $^{\circ}\text{C}$ and 334 $^{\circ}\text{C}$. The residual mass at 600 $^{\circ}\text{C}$ increases as the thiol content decreases, corresponding to a higher relative BisGMA content.

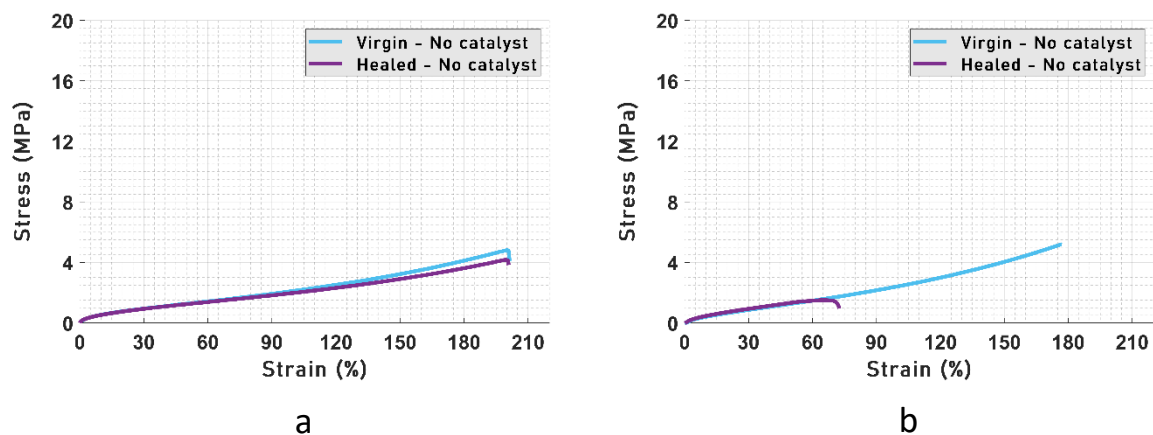


Fig. S8 – Tensile testing of non-catalysed SH14 samples. **(a)** 50 µm scratch size. Healing efficiency is 87%. **(b)** 150 µm scratch size. Healing efficiency amounts to 29%.

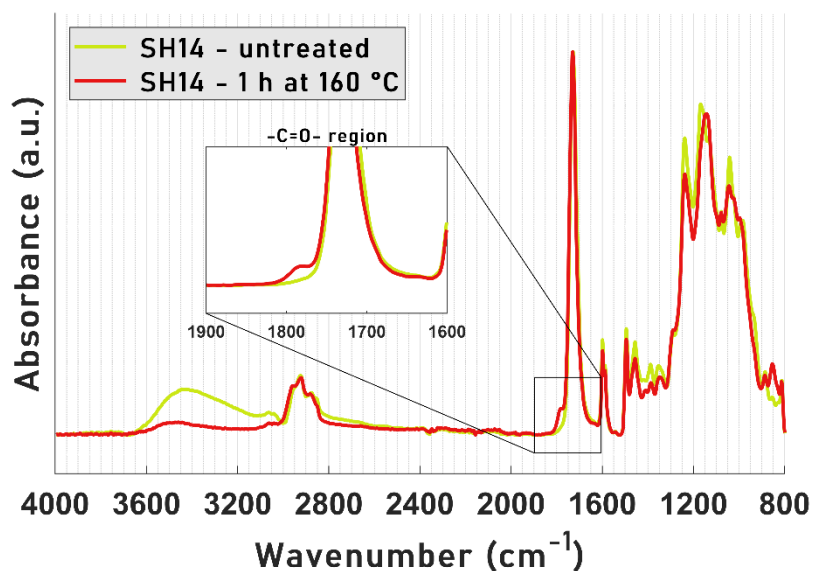


Fig. S9 – FTIR absorbance spectra of SH14 resin untreated (yellow) and thermally treated at 160 °C for 1 h (red). The inset zooms in the carbonyl bond region, where a small shoulder around 1800 cm⁻¹ is visible. This is a clear indication of hydrogen bonding formed in the presence of Miramer A99.

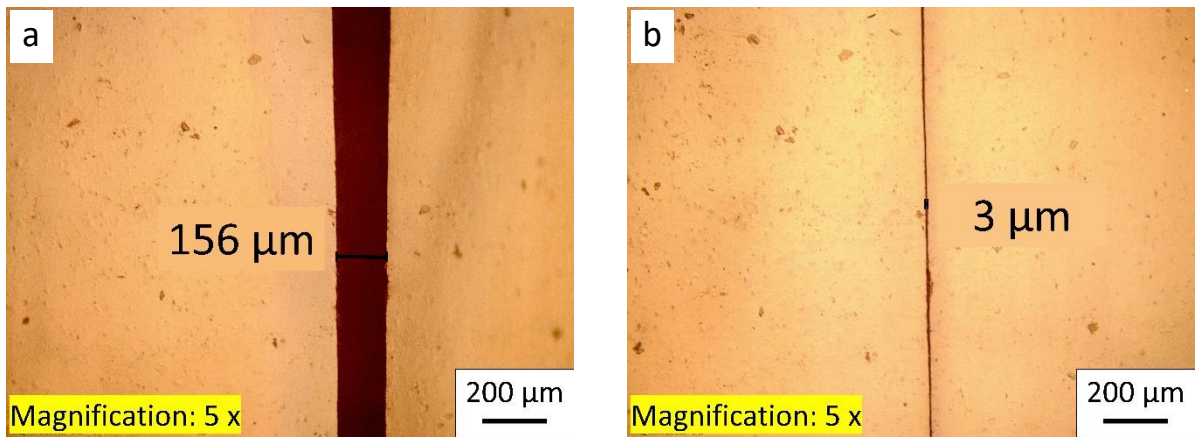


Fig. S10 – Shape memory-assisted closure of SH14 with larger scratch size (produced with the blade in Fig. S3b). **(a)** Sample scratched in the temporary stretched shape. **(b)** Sample after shape recovery. It is possible to observe a conspicuous scratch closure.

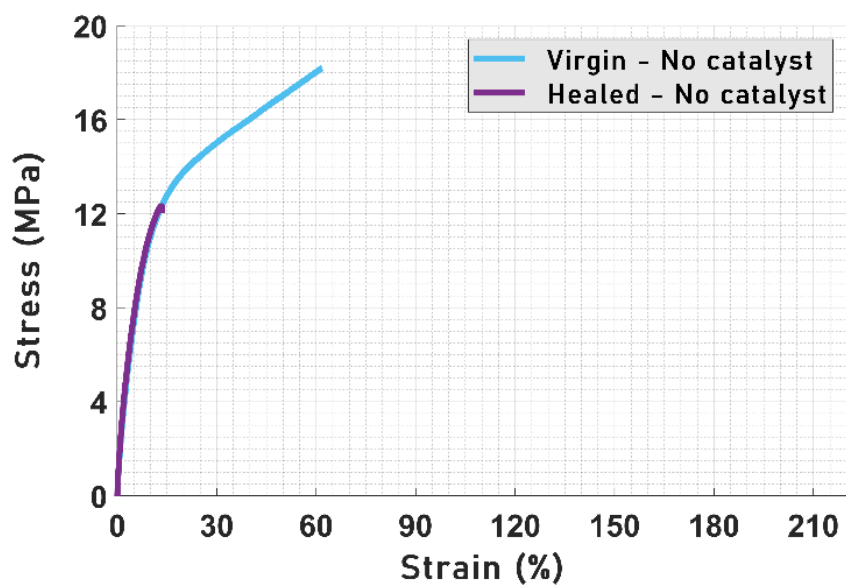


Fig. S11 – Stress-strain curves of non-catalysed SH7 samples. Based on ultimate tensile strength (UTS), the healing efficiency is 68%.

2. Calculations

Example of mathematical steps for the determination of T_v of thiol-ene SH14 network

From the DMA curves, the storage modulus E' in the rubbery plateau settled to an average value of 1.6062 MPa. Assuming incompressibility (Poisson's ratio $\nu = 0.5$) and by exploiting the relation between storage young's modulus and shear modulus G' , we calculated G' as:

$$G' = \frac{E'}{2(1 + \nu)} = \frac{1.6062}{2 \cdot (1 + 0.5)} \text{MPa} = 0.5354 \text{MPa}$$

We then calculated τ^* from Maxwell model, assuming that T_v corresponds to a viscosity $\eta = 10^{12} \text{Pa}\cdot\text{s}$:

$$\tau^* = \eta / G' = \frac{10^{12} \text{Pa}\cdot\text{s}}{0.5354 \cdot 10^6 \text{Pa}} = 1.868 \cdot 10^6 \text{s}$$

From the Arrhenius equation, we then extract T_v .

$$\ln(\tau^*) = \frac{E_a}{RT_v} + c = \frac{E}{R} \cdot \frac{1000}{T_v} + c$$
$$y = m \cdot x + c$$

E/R and c are the slope (m) and y-intercept of the linear fitting (i.e. Arrhenius plot) respectively.

$$\frac{1000}{T_v} = \frac{(\ln(\tau^*) - c)}{m} = \frac{14.44 - (-11.11)}{8.862} = 2.8831 \text{K}^{-1}$$

$$T_v = \frac{1000}{2.8831} - 273.15 = 74 \text{ }^\circ\text{C}$$

With an additional step, one can estimate the activation energy of the system:

$$E_a = 1000 \cdot m \cdot R = 1000 \cdot 8.862 \text{K}^{-1} \cdot 8.314 \text{J mol}^{-1}\text{K}^{-1} = 73.7 \text{kJ mol}^{-1}$$

3. References

1. G. Socrates, Infrared and Raman characteristic group frequencies: Tables and charts / George Socrates, Wiley, Chichester, 2001.
2. M. Capelot, M. M. Unterlass, F. Tournilhac and L. Leibler, ACS Macro Lett., 2012, **1**, 789.